Short communication

Fabrication of all solid-state lithium-ion batteries with three-dimensionally ordered composite electrode consisting of $Li_{0.35}La_{0.55}TiO_3$ and $LiMn_2O_4$

Masanori Hara [a], Hiroyuki Nakano [a,b], Kaoru Dokko [c], Sayaka Okuda [a], Atsushi Kaeriyama [a], Kiyoshi Kanamura [a,b,*]

[a] Department of Applied Chemistry, Tokyo Metropolitan University, 1-1 Minami-ohsawa, Hachioji, Tokyo 192-0397, Japan
[b] CREST, Japan Science and Technology Agency, 4-1-8 Honcho, Kawaguchi, Saitama 332-0012, Japan
[c] Department of Chemistry and Biotechnology, Yokohama National University, 79-5 Tokiwadai, Hodogaya-ku, Yokohama 240-8501, Japan

ARTICLE INFO

ABSTRACT

A composite electrode between three-dimensionally ordered macroporous (3DOM) $Li_{0.35}La_{0.55}TiO_3$ (LLT) and $LiMn_2O_4$ was fabricated by colloidal crystal templating method and sol–gel process. A close-packed PS beads with the opal structure was prepared by filtration of a suspension containing PS beads. Li–La–Ti–O sol was injected by vacuum impregnation process into the voids between PS beads, and then was heated to form 3DOM-LLT. Three-dimensionally ordered composite material consisting of $LiMn_2O_4$ and LLT was prepared by sol–gel process. The prepared composite was characterized with SEM and XRD. All solid-state Li-ion battery was fabricated with the LLT–$LiMn_2O_4$ composite electrode as a cathode, dry polymer electrolyte and Li metal anode. The prepared all solid-state cathode exhibited a volumetric discharge capacity of 220 mAh cm^{-3}.

1. Introduction

Lithium-ion battery system is one of the most attractive energy sources for mobile devices, emergency power supply systems, and hybrid electric vehicles, due to its high energy density. However, safety is one of the remaining problems for commercial lithium-ion batteries [1]. The all solid-state rechargeable lithium battery with a solid electrolyte is recognized as one of alternative technologies for rechargeable power source, because of likely higher energy density and improved safety. Polymer electrolytes [2–6] and ceramic electrolytes [7–15] have been extensively studied to eliminate flammable components in rechargeable lithium-ion batteries. Higher lithium-ion conductivity than 10^{-3} S cm^{-1} is required for practical rechargeable lithium batteries. Ceramic electrolytes have an advantage in a sense of non-flammable electrolyte as well as high ionic conductivity ($\sigma = \sim 10^{-3}$ S cm^{-1} at room temperature) with high Li-ion transport number ($t \approx 1.0$).

The problem for realizing all solid-state lithium-ion battery using the ceramic electrolyte is high internal resistance because of a poor contact between solid electrolyte and active material [16,17]. To fabricate a high performance electrode for all solid-state rechargeable Li batteries, the solid electrolyte-active material interface should be enlarged. We have proposed a novel electrode system using ceramic electrolyte with three-dimensionally ordered macroporous (3DOM) structure, which has a large surface area [18–21]. A large contact area between active material and ceramic electrolyte can be obtained by injecting an active material into the macropore of 3DOM ceramic electrolyte. We have already fabricated 3DOM solid electrolytes of $Li_{0.35}La_{0.55}TiO_3$ (LLT) and $Li_{1.5}Al_{0.5}Ti_{1.5}(PO_4)_3$ (LATP) using colloidal crystal templating method [18–21] and also fabricated composite electrodes consisting of 3DOM solid electrolytes and active materials [19,21]. It was reported that lithium-ion conductivities of LLT and LATP were high enough for practical rechargeable lithium batteries, 10^{-3} S cm^{-1} for LLT [7] and 1.3×10^{-3} S cm^{-1} for LATP [13]. However, the redox reaction of $Ti^{3+/4+}$ took place at 1.8 and 2.5 V versus Li/Li^+ on LLT and LATP, respectively. These electrochemical windows were limited by titanium redox reaction. Macropores in a 3DOM solid electrolyte interconnect each other, therefore, if the macropores are completely filled with an active material having electronic conductivity, 3D electronic conduction path can be formed in the composite. However, it was difficult to fill the macropore with active material sufficiently in our previous study. The filling ratio of active material in the 3DOM membrane was up to ~60%, and

* Corresponding author at: Department of Applied Chemistry, Tokyo Metropolitan University, 1-1 Minami-ohsawa, Hachioji, Tokyo 192-0397, Japan.
Tel.: +81 42 677 2828; fax: +81 42 677 2828.
E-mail address: kanamura@tmu.ac.jp (K. Kanamura).

voids still remained in the composite electrode [21]. The voids in the composite electrode system break down electron conduction paths, therefore some parts of active material were isolated electrically from the current collector. This results in lowering of utilization of the active material. By increasing the filling ratio of active material in the pore, the utilization of the electrode will be improved.

In this paper, the composite electrode consisting of 3DOM-LLT and $LiMn_2O_4$, was fabricated by sol–gel process, and was applied to cathode for all solid-state Li-ion battery. The electrochemical performance of all solid-state cell composed of solid polymer electrolyte, the composite electrode system between 3DOM-LLT and $LiMn_2O_4$ and Li metal anode was investigated.

2. Experimental

2.1. Fabrication of the composite between 3DOM-LLT and $LiMn_2O_4$

LLT with an inverse opal structure was prepared by colloidal crystal templating method using mono-dispersed polystyrene (PS) beads (3 μm in diameter, MAGSPHERE Inc.) and sol–gel process. The Li–La–Ti–O sol as a precursor of LLT was prepared from lithium acetate (98%), lanthanum acetate (99.99%), titanium tetraisopropoxide (97%), acetic acid (99.9%), 2-propanol (99.9%), and water. The molar ratio of lithium acetate, lanthanum acetate, titanium tetraisopropoxide, 2-propanol, acetic acid, and water was 0.35:0.55:1:20:10:140. Preparation method of 3DOM-LLT was described in detail in our previous paper [18,19]. Briefly, the PS beads suspended in water were filtered under a small pressure difference of 5 kPa using polycarbonate filter (0.1 μm in pore size, ADVANTEC) to obtain a template membrane with a opal structure, which had ideally 26% free space in volume between beads. After the filtration, the PS beads were interconnected by heat treatment at 110 °C for 1 h. The Li–La–Ti–O sol was injected into the PS template using vacuum impregnation and converted to gel under vacuum at room temperature. After gelation of the Li–La–Ti–O sol, the composite of ordered PS and Li–La–Ti–O gel was calcined at 450 °C for 1 h to remove PS beads and at 1000 °C for 1 h to crystallize LLT. After the heat treatment, crystallized porous LLT membrane was obtained.

The pores of porous LLT were filled with $LiMn_2O_4$ by sol–gel method. Lithium acetate as a Li source, manganese acetate tetrahydrate as a Mn source, 2-propanol, acetic acid, and water were mixed to prepare a precursor sol of Li–Mn–O. The molar ratio of these starting compounds was 1.1:2:40:20:70. Before impregnation of Li–Mn–O sol, the pore of 3DOM-LLT was filled with 0.02 M sodium dodecyl sulfate (SDS) solution. The 3DOM-LLT filled with SDS solution was immersed in the precursor sol for 1 h to inject the sol into the pore of 3DOM-LLT. The SDS solution in the macropores was replaced with Li–Mn–O sol during the immersion. After the immersion, the LLT membrane was lifted up from the sol solution, and the Li–Mn–O sol involved in the LLT porous membrane was converted to gel at 60 °C. The LLT–gel composite was calcined at 450 °C for 30 min. Since the Li–Mn–O gel contains a large amount of solvent and organic compounds, voids remain as results of evaporation of the solvent and decomposition of organic species during the heat treatment. In order to increase the filling ratio of active material in the pore of 3DOM solid electrolyte, the injection of Li–Mn–O sol and the following heat treatment was repeated four times. Finally, the composite was calcined at 700 °C for 10 h.

The prepared 3DOM LLT and the composite was observed with scanning electron microscope (SEM, JED-2100, JEOL Co.), and analyzed with X-ray diffraction method (XRD, RINT-UltimaII, Rigaku Co.).
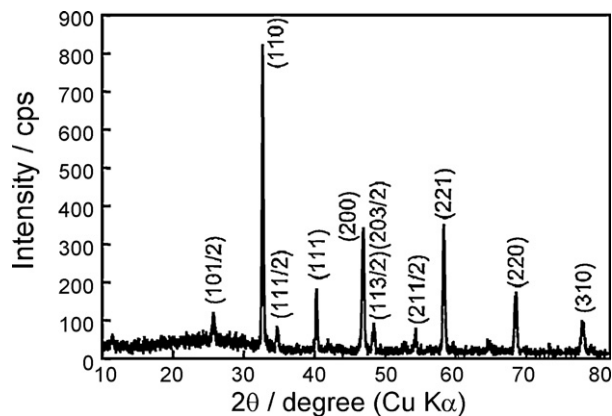

Fig. 1. XRD pattern of three-dimensionally ordered macroporous (3DOM) $Li_{0.35}La_{0.55}TiO_3$ (LLT) prepared at 1000 °C.

2.2. Charge–discharge property of LLT–$LiMn_2O_4$ composite electrode

The electrochemical property of the LLT–$LiMn_2O_4$ composite electrode was investigated by charge–discharge test with polymer electrolyte and Li anode. A block copolymer consisting of a polyethylene oxide and polystyrene containing 5 mol% lithium (bis(perfluoroethylsulfonyl)) imide (LiBETI) (Nippon Soda Co., Ltd.) was used as the polymer electrolyte. The property and preparation method of the block copolymer used in present study was described in detail in our previous papers [2–4]. All solid-state Li-ion battery for evaluation of the composite between 3DOM-LLT and $LiMn_2O_4$ was fabricated as follows. Au was sputtered on one face of the composite to obtain an electrical contact between the composite and Al current collector. Then the block copolymer containing LiBETI dissolved in dimethoxyethane was cast on the composite cathode, and the solvent of the polymer solution was evaporated by holding it under weak reduced pressure (−30 kPa) for 10 min. After repeating this process several times, the polymer electrolyte was dried at 85 °C under vacuum for 5 h to remove the solvent. Li metal foil as an anode was put on the electrolyte film, and Cu foil was used as a current collector for Li electrode. The all solid-state cell with the dry polymer electrolyte for electrochemical measurement was fabricated by sandwiching the cell assembly by using two polypropylene plates fixed by double clips. The charge and discharge tests were measured by using a dc power supply (HJR-110mSM6, HOKUTO DENKO) under Ar atmosphere at room temperature. The cell was charged to 4.3 V and discharged to 3.0 V at a constant current of 25 μA cm^{-2}.

3. Results and discussion

Fig. 1 shows the XRD patterns of 3DOM-LLT prepared at 1000 °C. The indexing of XRD patterns was based on cubic perovskite lattice. It was confirmed that the obtained LLT had a perovskite-type structure. Low intensity of diffraction peaks was due to the high porosity of the LLT membrane. The porosity of the 3DOM membrane was estimated to be 70% from the dimensions and weight of the membrane, which was almost identical to the theoretical value (74%).

A cross-sectional SEM image of 3DOM-LLT before impregnation of active material is shown in Fig. 2(a). The macropore size was ca. 2 μm, which was smaller than that of the PS beads used as template (3 μm), indicating that the shrinkage of the 3DOM-LLT took place during heat treatment. Interconnecting window was observed on entire part of the LLT membrane. The ionic conductivity of 3DOM-LLT estimated by AC impedance measurement over
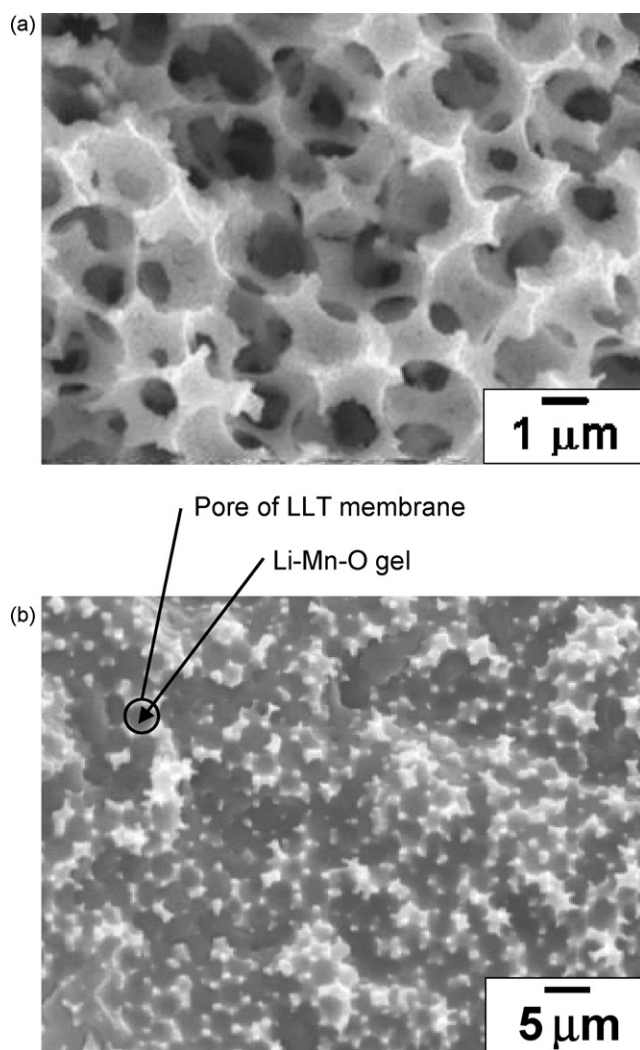
Fig. 2. Cross-sectional SEM images of the 3DOM-LLT membrane: (a) before and (b) after filling with Li–Mn–O gel.
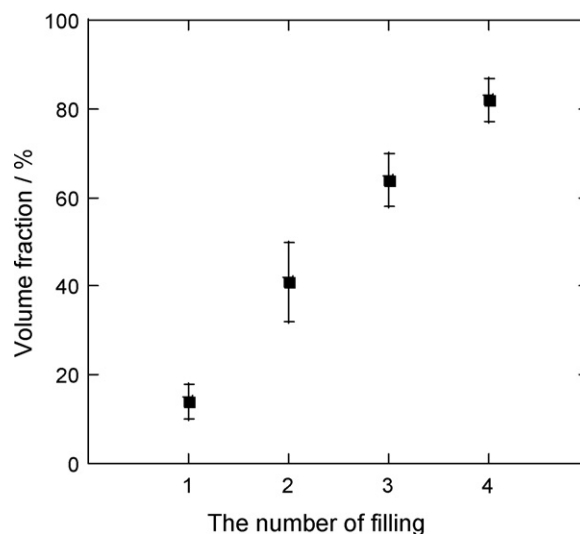

Fig. 3. Plot of volume fraction of $LiMn_2O_4$ referred to volume of the pores versus repeating number of filling the 3DOM-LLT membrane with active material.

the frequency range from 13 MHz to 5 Hz has been already reported in our previous papers [18]. Silver paste was utilized to obtain electrical contact from the sample. The conductivity of 3DOM-LLT, ca. $2.1 \times 10^{-4}\,S\,cm^{-1}$, was lower than the reported value ($>10^{-3}\,S\,cm^{-1}$) [7], because of defects in the 3DOM-LLT, which break down a part of ion conduction network.

Fig. 2(b) shows the cross-sectional SEM image of 3DOM-LLT after the injection and gelation of Li–Mn–O sol into the LLT membrane. In Fig. 2(b), bright area with circle shape corresponds to 3DOM-LLT, and gray color area was Li–Mn–O gel impregnated into the pores of the LLT membrane. It can be seen the pores of 3DOM-LLT are almost completely filled up with Li–Mn–O gel. In our previous study, we injected precursor of active material into pores by vacuum impregnation process without SDS solution. However, it was difficult to fill up the 3DOM-LLT fully with the Li–Mn–O sol, because of small pore and interconnect window size, high viscosity of the sol, as well as gelation during impregnation of the sol under vacuum [19]. On the other hand, it was possible to inject Li–Mn–O sol sufficiently into the pores of LLT in the present study. Prior to the injection of Li–Mn–O sol, the pores of LLT membrane were filled with SDS solution as mentioned in Section 2. Fig. 2(b) demonstrates that the pre-treatment of the LLT membrane by SDS solution improves the filling ratio of the Li–Mn–O gel. It was considered that the pre-treatment was effec-

tive in improving the wettability of LLT to Li–Mn–O sol, which resulted in increasing the filling ratio of gel in the 3DOM membrane. We fabricated three-dimensionally ordered composite electrode using 3DOM-LLT and $LiMn_2O_4$ by heat treatment of the composite between 3DOM-LLT and Li–Mn–O gel. The volume fraction of $LiMn_2O_4$ referred to volume of the pores in the membrane was plotted versus repeating number of Li–Mn–O sol injection and following heat treatment (Fig. 3). The volume of the pores was estimated from volume and weight of 3DOM-LLT membrane without $LiMn_2O_4$. The volume fraction of $LiMn_2O_4$ was determined from weight change of the composites between LLT–$LiMn_2O_4$ during repeat of the sol impregnation. The plot shows that the volume fraction was increased linearly with repeating the injection of Li–Mn–O sol. The result indicates that the filling ratio of the active material in the pore of 3DOM solid electrolyte can be increased by repeating the impregnation of the sol. After repetition of the impregnation four times, the volume fraction of $LiMn_2O_4$ in 3DOM-LLT membrane reached to ca. 80%, which is relatively high volume fraction for the composite as the cathode material. Further repeating of the impregnation caused the deposition of $LiMn_2O_4$ not only on the inside of the pores but also on membrane surface. The LLT–$LiMn_2O_4$ composite membrane with the volume fraction of ca. 80% was used for charge–discharge test to avoid peeling of $LiMn_2O_4$ from LLT and fragmentation of the composite, which are caused by the volume change of active material, $LiMn_2O_4$, during Li deintercalation/intercalation cycle.

Fig. 4(a) and (b) shows SEM images of the composite electrode between 3DOM-LLT and $LiMn_2O_4$ after first and fourth sol injection and the following heat treatment at 450 and 700 °C, respectively. By comparing the SEM image of the composite electrode system (Fig. 4) with that of 3DOM-LLT (Fig. 2(a)), it was found that $LiMn_2O_4$ was injected into the pore of 3DOM-LLT. Although 3DOM-LLT was filled up with the Li–Mn–O gel with SDS pre-treatment, as shown in Fig. 2(b), voids were still observed in the composite electrode after the heat treatment at 450 °C (Fig. 4(a)). This is due to a large amount of solvent contained in the Li–Mn–O gel injected into the pore of 3DOM-LLT. The decreasing of the remaining voids in the composite after the impregnation for the Li–Mn–O sol four times, as shown in Fig. 4(b), are consistent with the volume fraction increase with repeating the injection of Li–Mn–O sol mentioned above.

The XRD pattern of the composite of 3DOM-LLT and $LiMn_2O_4$ after final heat treatment at 700 °C is shown in Fig. 5. The diffraction peaks were assigned to those of $LiMn_2O_4$ with spinel structure
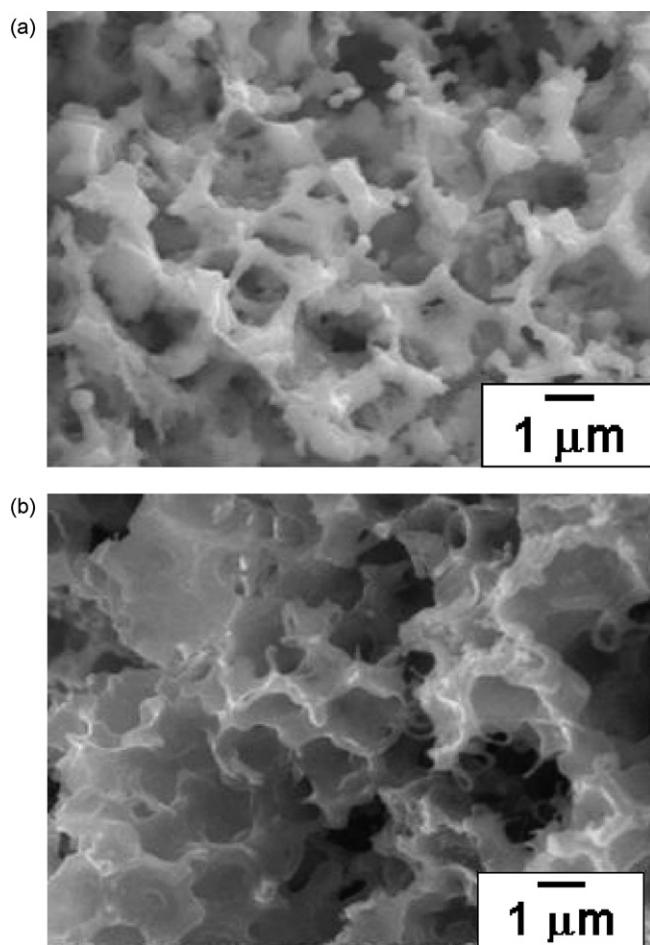
Fig. 4. Cross-sectional SEM images of the composite electrode system between 3DOM-LLT and $LiMn_2O_4$ with different $LiMn_2O_4$ volume fraction: (a) 13% and (b) 80%.

and LLT with perovskite-type structure [19]. No diffraction peak assigned to impurities was observed. It was confirmed that the injection and the calcination of $LiMn_2O_4$ did not provide any impurities in 3DOM-LLT. In this way, the composite electrode between 3DOM-LLT and $LiMn_2O_4$ was successfully fabricated.

Fig. 6 shows the charge–discharge curves of all solid-state cell with the composite electrode system between 3DOM-LLT and $LiMn_2O_4$. The potential plateaus due to redox reaction of $Mn^{3+/4+}$ in $LiMn_2O_4$ were observed around 4.0 V. The result indicates that Li deintercalation/intercalation from/into $LiMn_2O_4$ take place at the interface of $LiMn_2O_4$–LLT solid electrolyte. The first
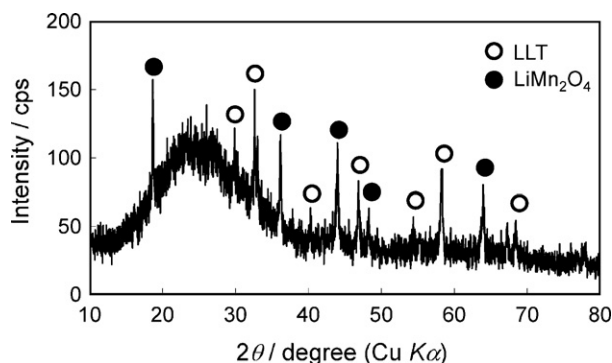

Fig. 5. XRD pattern of the composite electrode consisting of LLT and $LiMn_2O_4$ after final heat treatment at 700 °C.
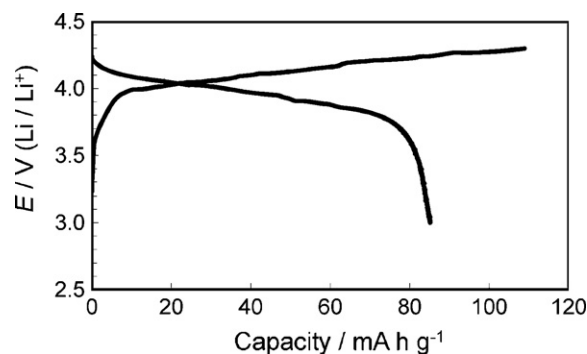

Fig. 6. Charge–discharge curves of the LLT–$LiMn_2O_4$ composite as cathode for all solid-state cell at 0.016 C rate (25 $\mu A\,cm^{-2}$).

discharge capacity was 83 mAh g^{-1}, which was lower than the theoretical value (148 mAh g^{-1}). However, the volumetric capacity of the LLT–$LiMn_2O_4$ composite exhibited relatively high capacity of 220 mAh cm^{-3}, which was comparable to a volumetric capacity of $LiMn_2O_4$ electrode used in a Li-ion battery with liquid electrolyte. The coulombic efficiency of the composite electrode was 75% at the first charge–discharge cycle. The low coulombic efficiency was due to the low conductivity of the prepared cell with LLT–$LiMn_2O_4$ composite and/or degradation of the 3DOM structure by volume change of the active material during charge–discharge cycle. Probably, the low ionic conductivity of LLT and polymer electrolyte as well as poor conductivities of LLT–$LiMn_2O_4$ and LLT–polymer electrolyte interfaces resulted in larger polarization compared with that of liquid electrolyte system. Unfortunately, in the case of all solid-state cell comprising Li/polymer electrolyte/3DOM LLT–$LiMn_2O_4$ composite, the estimation of the conductivity of 3DOM LLT–$LiMn_2O_4$ and LLT–polymer electrolyte of the prepared cell was difficult, because these AC impedances were observed in similar frequency range. In order to evaluate the resistances of the interface between LLT and $LiMn_2O_4$, and between LLT and polymer electrolyte individually, thin-film electrode of $LiMn_2O_4$ formed on a dense pellet of LLT as well as polymer-electrolyte-modified LLT pellet were fabricated. The impedance measurements for Li/PMMA electrolyte/LLT pellet/$LiMn_2O_4$ thin-film and Au/LLT pellet/polymer electrolyte/Li were carried out. From the results of impedance measurements (not shown here), it was considered that the resistance of the interface between LLT pellet and $LiMn_2O_4$ thin-film was larger than that of LLT–polymer electrolyte interface. The interfacial resistance between LLT and $LiMn_2O_4$ thin film was about 5 kΩ cm^2, which was more than 10 times larger than that of LLT–polymer interface, which was ca. 400 Ω cm^2. In fact, similar results were obtained for the cell consisting of Li/PMMA electrolyte/$Li_{1+x}Al_xTi_{2-x}(PO_4)_3$ solid electrolyte/$LiMn_2O_4$ thin-film electrode in our previous study [17]. Further studies on the interface between LLT and $LiMn_2O_4$ cathode are underway in our group and will be reported in due course.

4. Conclusion

The novel electrode system composed of 3DOM-LLT and $LiMn_2O_4$ was successfully prepared by colloidal crystal templating method and sol–gel process. The composite of 3DOM-LLT and $LiMn_2O_4$ was fabricated by the injection of Li–Mn–O sol into the macropore of 3DOM-LLT and following heat treatment. The formation of the composite between 3DOM-LLT and $LiMn_2O_4$ were confirmed with SEM and XRD. The crystallographic structure of LLT and $LiMn_2O_4$ in the LLT–$LiMn_2O_4$ composite electrode was assigned to perovskite and spinel structure, respectively. Furthermore, the composite electrode between 3DOM-LLT and $LiMn_2O_4$, which was

used as the positive electrode system for all solid-state Li-ion battery, was evaluated by charge and discharge test. The volumetric discharge capacity of the composite electrode was 220 mAh cm^{-3}.

References

[1] J.M. Tarascon, M. Armand, Nature 414 (2001) 359.
[2] T. Niitani, M. Shimada, K. Kawamura, K. Kanamura, J. Power Sources 146 (2005) 386.
[3] T. Niitani, M. Simada, K. Kawamura, K. Dokko, Y.H. Rho, K. Kanamura, Electrochem. Solid State Lett. 8 (2005) A385.
[4] H. Nakano, K. Dokko, J. Sugaya, T. Yasukawa, T. Matsue, K. Kanamura, Electrochem. Commun. 9 (2007) 2013.
[5] Y. Masuda, M. Nakayama, M. Wakihara, Solid State Ionics 178 (2007) 981.
[6] F. Croce, F. Serraino Fiory, L. Persi, B. Scrosati, Electrochem. Solid State Lett. 4 (2001) A121.
[7] Y. Inaguma, C. Liquan, M. Itoh, T. Nakamura, T. Ichida, H. Ikuta, M. Wakihara, Solid State Commun. 86 (1993) 689.
[8] T. Abe, M. Ohtsuka, F. Sagane, Y. Iriyama, Z. Ogumi, J. Electrochem. Soc. 151 (2004) A1950.
[9] H. Aono, E. Sugimoto, Y. Sadaoka, N. Imanaka, G. Adachi, J. Electrochem. Soc. 136 (1989) 590.
[10] H. Aono, E. Sugimoto, Y. Sadaoka, N. Imanaka, G. Adachi, J. Electrochem. Soc. 137 (1990) 1023.
[11] K. Takada, M. Tansho, I. Yanase, T. Inada, A. Kajiyama, M. Kouguchi, S. Kondo, M. Watanabe, Solid State Ionics 139 (2001) 241.
[12] M. Cretin, P. Fabry, J. Eur. Ceram. Soc. 19 (1999) 2931.
[13] J. Fu, Solid State Ionics 96 (1997) 195.
[14] A. Hayashi, T. Konishi, K. Tadanaga, M. Tatsumisago, Solid State Ionics 177 (2006) 2737.
[15] R. Murugan, V. Thangadurai, W. Weppner, Angew. Chem. Int. Ed. 46 (2007) 7778.
[16] K. Hoshina, K. Dokko, K. Kanamura, J. Electrochem. Soc. 152 (2005) A2138.
[17] K. Dokko, K. Hoshina, H. Nakano, K. Kanamura, J. Power Sources 174 (2007) 1100.
[18] K. Dokko, N. Akutagawa, Y. Isshiki, K. Hoshina, K. Kanamura, Solid State Ionics 176 (2005) 2345.
[19] K. Kanamura, N. Akutagawa, K. Dokko, J. Power Sources 146 (2005) 86.
[20] Y. Isshiki, K. Dokko, K. Kanamura, J. Jpn. Soc. Powder Powder Metall. 53 (2006) 856.
[21] H. Nakano, K. Dokko, M. Hara, Y. Isshiki, K. Kanamura, Ionics 14 (2008) 173.